Analysis of Partial Relay Selection in NOMA Systems with RF Energy Harvesting

Le The Dung*, Tran Manh Hoang†, Nguyen Trung Tan†, Seong-Gon Choi*
*Department of Radio and Communication Engineering, Chungbuk National University, Korea.
Emails: dung.t.le@ieee.org, sgchoi@cbnu.ac.kr
†Faculty of Radio Electronics, Le Quy Don Technical University, Vietnam.
Emails: tranmanhhoang@tcu.edu.vn, trungtan68@gmail.com

***Abstract*—In this paper, we investigate a dual hop communication decode-and-forward relaying system where a source node wants to transmit two symbols to its two desired destinations with the help of a selected energy constraint relay node. The power for relay operation comes from the harvested energy of ambient radio frequency (RF) and the non-orthogonal multiple access (NOMA) technology is used. We mathematically evaluate the impact of relay selection (RS) on the system performance by considering the probability that symbols cannot be decoded at the two end users under the effect of imperfect and perfect successive interference cancellation (SIC). We also perform Monte-Carlo simulations in MATLAB to verify the correctness of our analysis. The results show that the performance of the system is significantly influenced by the efficiency of SIC technique. Moreover, if the power transmission is in high region, we can use approximation method to simplify our analysis.**

***Index Terms*—NOMA, Partial Relay Section, Energy Harvesting, Perfect and Imperfect Successive Interference Cancellation.**

I. Introduction

Non-orthogonal multiple access (NOMA) has been proven as a promising technique for the fifth generation (5G) mobile networks due to its superior spectral efficiency [1]. Unlike orthogonal-multiple-access (OMA), NOMA allows multiple users to pair and share the same radio resources such as time, frequency, and code. The key idea of NOMA is to explore power domain, where users are served at different power levels [2]. More importantly, NOMA has recently been recognized as a promising multiple access (MA) technique to significantly improve the spectral efficiency of mobile communication networks. It is also been envisioned as the key component in fifth generation (5G) mobile systems.

NOMA has also been applied to cooperative relaying systems [3], [4]. In [3], the cooperative NOMA system with buffer-aided relaying is studied. Assuming that the relay node possesses a buffer, the authors propose an adaptive transmission scheme in which the system adaptively chooses its working mode in each time slot. The authors of [4] propose and investigate a dual-hop cooperative relaying scheme using NOMA, where two sources communicate with their corresponding destinations simultaneously over the same frequency band and via a common relay. After receiving symbols transmitted from both sources with different allocated power levels, the relay forwards a superposition coded composite signal to the destinations by using NOMA technique. The NOMA systems with RF harvested energy are investigated in [5]–[7]. A system in which near NOMA users to the source act as energy harvesting relays to help far NOMA users is analyzed in [8]. This system utilizes an energy havesting technology called simultaneous wireless information and power transfer (SWIPT). All users are spatial randomly located.

The SWIPT is an emerging energy harvesting technology. Despite its advantages, there remains considerable lack of studying the joint effect of SWIPT and NOMA relaying systems in the literature. Existing works only focus on deriving the outage performance of NOMA-EH relaying networks with antenna selection and single relay. The most related to our work is selecting antenna at the source and splitting power at the relay which is presented in [7]. To the best of our knowledge, the aforementioned works have not discussed the energy harvesting combined with the partial relay selection and NOMA technique. The main contributions of this paper are summarized as follows:

- We propose a NOMA system where the relay node harvests the energy from the radio frequency by using time switching scheme to support forwarding information to both two users.
- We evaluate the performance of partial selection relay scheme by deriving the closed-form expression of the probability that desired information at the best relay node and destination nodes cannot be decoded successfully.
- We compare the performance of NOMA-EH system under the influence of imperfect SIC and perfect SIC. We prove that the level of residual interference of the imperfect SIC significantly impacts on the probability of unsuccessful decoding symbol x_2.

The rest of this paper is organized as follows. Section II describes the system model of partial relay selection in NOMA system with RF energy harvesting. The mathematical analysis of the system is presented in Section III. Numerical results are shown in Section IV to show the performance of our proposed system. Finally, the paper is concluded in Section V.

II. System Model

We consider a NOMA downlink system comprised of one source (S), two users D_1 and D_2 as illustrated in Fig. 1. Due to far distance or deep shadow-fading, the direct link is

978-1-5386-2976-5/18/$31.00 ©2018 IEEE

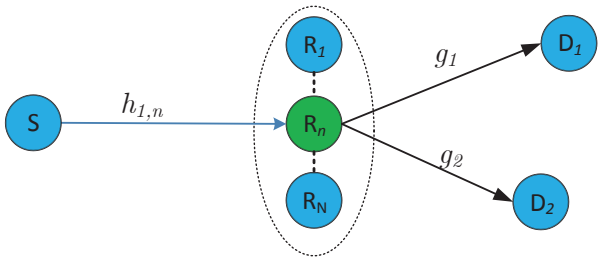

Fig. 1. Partial relaying selection in NOMA downlink relay network with RF energy harvesting.

assumed not available. Thus, the communication of the system is assisted by several relay nodes R_n where $n \in \{1, ..., N\}$. In this paper, we only consider the case of partial relay selection. It is also assumed that every node is equipped with single antenna and operates in a half-duplex mode. Moreover, all relays have no fixed power supply but are powered by the wireless energy transfer from the source. The channels from S to R_n and from R_n to D_i exhibit frequency, non-selective Rayleigh block fading.

As shown in Fig. 1, $h_{SR_n} \sim CN(0, \lambda_{1,n})$ is the complex channel coefficient between S and R_n. $\mathrm{w_R} \sim CN(0, 1)$ is the additive white Gaussian noise (AWGN). $g_i \sim CN(0, \lambda_{R_n D_i})$ and w_{D_i} denote the complex channel coefficient and the AWGN between to R_n and to D_i, $i \in \{1, 2\}$, respectively. Since the path loss and shadowing effect of g_1 are more severe than g_2, we have $\lambda_{R_n D_1} < \lambda_{R_n D_2}$ which is important for performing the successive interference cancellation (SIC) [9]. In addition, we assume the CSI is available at any terminal in the network.

In this paper, we consider the relay selection scheme where the relay node is selected based only on the instantaneous knowledge of the channel pertaining to the first hop. The source terminal continuously monitors the quality of its connectivity with the relays via the transmission of local feedbacks. From this information, the source selects the best link $\mathrm{S} \to \mathrm{R}_n$ for data transmission. As multiple relay nodes form a group, one best relay R_b is selected before transmitting. This partial relay selection strategy is expressed as

$$R_b = \arg \max_{n=1,2\cdots,N} |h_{1,n}|^2. \tag{1}$$

We assume that almost harvested power is consumed by the relays for forwarding signals to D_1 and D_2. The processing power required for the transmitting - receiving circuitry of the relay is generally negligible compared to the power used for signal transmission.

The time switching (TS) architecture for harvesting energy [10][1] is applied. Specifically, the energy is harvested from the received information signal for a duration of αT in each block. α is the fraction of the block time in which the relay harvests energy from the received information signal. T is the block time in which a certain information is transmitted from source node to destination node. Hence, the harvested energy is given by [11].

$$E_h = \frac{\alpha T \eta P_{\mathrm{S}} |h_{1,n}|^2}{N_0}, \tag{2}$$

where η is the energy conversion efficiency. Depending on the quality of energy harvesting electric circuitry, $0 < \eta \leq 1$.

From (2), the transmission power of relay node is calculated as

$$\begin{aligned} P_{\mathrm{R}} &= \frac{E_h}{(1-\alpha)\,T/2} \\ &= \frac{2\alpha\eta P_{\mathrm{S}} |h_{1,n}|^2}{1-\alpha}. \end{aligned} \tag{3}$$

The operation on the system is briefly described as follows. There are two time slots involving in each transmission block. All blocks are normalized to one unit. During the first time slot, source node will transmit the superimposed mixture, where x_i and a_i denote the signal and the power allocation coefficient of user i, respectively. It should be noted that $a_1 + a_2 = 1$. Following the principle of NOMA, we assume that $a_1 \geq a_2$ if the QoS requirements of D_1 are higher than D_2 [12]. The baseband signal received at R_n is thus given by

$$y_{\mathrm{R}}^n = \sqrt{P_{\mathrm{S}}} h_{1,n} \left(\sqrt{a_1} x_1 + \sqrt{a_2} x_2\right) + \mathrm{w_R}, \tag{4}$$

where $h_{1,n}$ denotes the complex channel coefficient between source S and relay nth, P_{S} is transmission power of S. The messages to be received at D_1 and D_2 are x_1 and x_2, respectively.

Since the key idea of NOMA technique is to use the power domain for multiple accesses, i.e. users are served at different power levels, and to adopt the superposition code at the transmitter, we use the SIC principle to decode signals at the receivers. The stronger signal is decoded and removed from the superposed signals, so the decoding is only applied to the other signal. Accordingly, in this paper, we only consider SIC process at the best relay node and D_2 because D_1, which performs decoding first, had already obtained the information symbol x_1.

When SIC technique is employed at the R_n, the best relay R_b first decodes the symbol x_1 by treating the symbol x_2 as noise. Then, R_b performs SIC to obtain symbol x_2. Thus, the received signal-to-interference-plus-noise ratio (SINR) for symbol x_1 and signal-to-noise ratio (SNR) for symbol x_2 at R are written as

$$\gamma_{1,u1} = \frac{a_1 P_{\mathrm{S}} |h_{1,n}|^2}{a_2 P_{\mathrm{S}} |h_{1,n}|^2 + 1}. \tag{5}$$

$$\gamma_{1,u2} = a_2 P_{\mathrm{S}} |h_{1,n}|^2. \tag{6}$$

We assume that in the first time slot, R_n successfully processes messages x_1, x_2 and SIC is perfect, i.e, the level of residual interference is zero. In the second time slot, the

[1]The proposed analysis approach can be applied for the power spitting energy harvesting model.

selected relay sends a message $\sqrt{P_{\mathrm{R}}}\left(\sqrt{a_1}x_1+\sqrt{a_2}x_2\right)$ to two users D_1 and D_2. Hence, the signals received at D_i is

$$y_{\mathrm{D}_i}=\sqrt{P_{\mathrm{R}}}g_i\left(\sqrt{a_1}x_1+\sqrt{a_2}x_2\right)+\mathrm{w}_{\mathrm{D}_i}, \tag{7}$$

where g_i denotes the channel gain between the selected relay and D_i.

According to the SIC principle, D_1 first decodes symbol x_1 and treats x_2 as noise. From (4), the signal-to-interference-plus-noise ratio (SINR) at D_1 is given by

$$\gamma_{2,u_1}=\frac{a_1P_{\mathrm{R}}|g_1|^2}{a_2P_{\mathrm{R}}|g_1|^2+1}. \tag{8}$$

Similarly, D_2 can decode its own message with the SNR as

$$\gamma_{2,u_2}=a_2P_{\mathrm{R}}|g_2|^2. \tag{9}$$

It should be noticed that x_1 and x_2 coexist at D_2. Therefore, SIC is needed to decode own symbol x_2. To perform SIC, D_2 decodes high powered symbol x_1 by treating the low-power symbol x_2 as noise, and cancels it using SIC to obtain the symbol x_2. Thus, the received SINR for x_1 at D_2 is given by

$$\gamma_{2,u_1\to u_2}=\frac{a_1P_{\mathrm{R}}|g_2|^2}{a_2P_{\mathrm{R}}|g_2|^2+1}. \tag{10}$$

III. Performance Analysis

In this section, we will present the outage probability of the partial relay selection scheme in NOMA system with RF energy harvesting. The outage probability can be referred as the probability that symbols x_1 and x_2 are not able to be decoded at D_1 and D_2. We will use interchangeably the concepts of outage probability and the probability of failing to decode symbols.

A. Probability that symbol x_1 cannot be decoded

We denote $\mathrm{P}_{x_1}^{\mathrm{error}}$ as the event that best relay cannot decode x_1 or D_1 and D_2 cannot decode x_1 successfully. From (5), (8), and (10), we can write the expression of $\mathrm{P}_{x_1}^{\mathrm{error}}$ as in (11) shown on the top of the next page [13], where $\gamma_{\mathrm{th1}}=2^{(2R/1-\alpha)}-1$, R is the target data rate.

Let $|h_{1,n}|^2=X_i$, $|g_1|^2=Y$, and $|g_2|^2=Z$ be the channel gains from source S to the best relay and from the best relay to D_1 and D_2, respectively. When the partial relay selection is applied, we have $|h_1|^2=\arg\max_{n\in 1:N}|h_{1,n}|^2$. We can rewrite (11) to become (12) shown on the top of next page, where $\phi=\frac{2\alpha\eta}{1-\alpha}$. As can be seen from (12), the outage always occurs if $\gamma_{\mathrm{th1}}>\frac{a_1}{a_2}$. Hence, we need to allocate more power to D_1. In other words, $a_1>a_2\gamma_{th1}$ is required.

By using the conditional probability in [14], we can rewrite (12) as

$$\begin{aligned}\mathrm{P}_{x_1}^{\mathrm{erro}}&=1-\int_{t_1}^{\infty}\Pr\left\{Y>\frac{t_2}{x},Z>\frac{t_2}{x}\right\}f_X(x)\,dx\\&=1-\int_{t_1}^{\infty}\int_{\frac{t_2}{x}}^{\infty}\left[1-F_Y\left(\frac{t_2}{x}\right)\right]f_Z(z)\,f_X(x)\,dxdz.\end{aligned} \tag{13}$$

where $t_1=\frac{\gamma_{\mathrm{th1}}}{P_{\mathrm{S}}(a_1-a_2\gamma_{\mathrm{th1}})}$, $t_2=\frac{\gamma_{\mathrm{th1}}}{P_{\mathrm{S}}\phi(a_1-a_2\gamma_{\mathrm{th1}})}$, $f_X(x)$ and $f_Z(z)$ are the probability density functions (PDFs) of X and Z, repectively, $F_Y(y)$ is the cumulative distribution function (CDF) of Y.

In this paper, we assume that all channel coefficients are modeled as independent Rayleigh-distributed random variables (RVs). Therefore, RVs $|h_{1,n}|^2$, $|g_1|^2$, and $|g_2|^2$ have exponential distributions, with $f_X(x)=\sum_{n=1}^{N}(-1)^{n-1}\binom{N}{n}\frac{n}{\lambda_x}\exp\left(-\frac{nx}{\lambda_x}\right)$[2], $F_Y(y)=1-\exp\left(-\frac{y}{\lambda_y}\right)$, and $f_Z(z)=\frac{1}{\lambda_z}\exp\left(-\frac{z}{\lambda_z}\right)$.

Hence, from (13), we have

$$\mathrm{P}_{x_1}^{\mathrm{erro}}=1-\sum_{n=1}^{N}(-1)^{n-1}\binom{N}{n}\frac{n}{\lambda_x}\underbrace{\int_{t_1}^{\infty}\exp\left(-\frac{\beta}{x}-\frac{nx}{\lambda_x}\right)dx}_{\psi}, \tag{14}$$

where $\lambda_x=\mathrm{E}\{X\}$, $\lambda_y=\mathrm{E}\{Y\}$, $\lambda_z=\mathrm{E}\{Z\}$ are the means of random variables and $\beta=\frac{t_2}{\lambda_y}+\frac{t_2}{\lambda_z}$.

Unfortunately, it is impossible to derive the closed-form expression of ψ in (14), thus, we will employ the approximation method. By using the expanded Taylor's series, it follows that $\exp\left(-\frac{a}{x}\right)=\sum_{k=0}^{N_t}\frac{(-1)^k}{k!}\left(\frac{a}{x}\right)^k$, where $N_t\in\{1,\cdots,\infty\}$. Then, we obtain

$$\begin{aligned}\psi&=\sum_{k=0}^{N_t}\frac{(-1)^k}{k!}\int_{t_1}^{\infty}\left(\frac{\beta}{x}\right)^k\exp\left(-\frac{nx}{\lambda_x}\right)dx\\&=\sum_{k=0}^{N_t}\frac{(-1)^k\beta^k}{k!}\left(\frac{1}{t_1}\right)^{k-1}E_k\left(\frac{nt_1}{\lambda_x}\right).\end{aligned} \tag{15}$$

Substituting (15) into (14), we get the expression of $\mathrm{P}_{x_1}^{\mathrm{error}}$ as

$$\mathrm{P}_{x_1}^{\mathrm{error}}=1-\sum_{n=0}^{N}\sum_{k=0}^{N_t}\frac{(-1)^n(-1)^k\beta^k}{k!}\binom{N}{n}\frac{n}{\lambda_x}\left(\frac{1}{t_1}\right)^{k-1}E_k\left(\frac{nt_1}{\lambda_x}\right), \tag{16}$$

where $E_k(\cdot)$ is the exponential integral function [15].

As we can see from (14), if the power transmits lies in a high region, it will lead to $t_1=\frac{\gamma_{\mathrm{th1}}}{P_{\mathrm{S}}\approx\infty(a_1-a_2\gamma_{\mathrm{th1}})}\to 0$. Thus, we apply [15, (3.324.1)] to obtain the final expression of $\mathrm{P}_{x_1}^{\mathrm{error}}$ as

$$\mathrm{P}_{x_1}^{\mathrm{erro}}\approx 1-\sum_{n=1}^{N}(-1)^{n-1}\binom{N}{n}\sqrt{\frac{4n\beta}{\lambda_x}}K_1\left(\sqrt{\frac{4n\beta}{\lambda_x}}\right). \tag{17}$$

where $K_1(\cdot)$ is the first-order modified Bessel function of the second kind.

[2]The sequence of X are referred as the order statistics of the sequence of $X_{1,n}$.

$$\mathrm{P}_{x_1}^{\mathrm{error}} = 1 - \Pr\left\{ \frac{a_1 P_{\mathrm{S}} |h_{1,n}|^2}{a_2 P_{\mathrm{S}} |h_{1,n}|^2 + 1} > \gamma_{\mathrm{th1}}, \frac{a_1 P_{\mathrm{R}} |g_1|^2}{a_2 P_{\mathrm{R}} |g_1|^2 + 1} > \gamma_{\mathrm{th1}}, \frac{a_1 P_{\mathrm{R}} |g_2|^2}{a_2 P_{\mathrm{R}} |g_2|^2 + 1} > \gamma_{\mathrm{th1}} \right\}, \tag{11}$$

$$\mathrm{P}_{x_1}^{\mathrm{error}} = 1 - \Pr\left\{ X > \frac{\gamma_{\mathrm{th1}}}{P_{\mathrm{S}}\left(a_1 - a_2\gamma_{\mathrm{th1}}\right)}, XY > \frac{\gamma_{\mathrm{th1}}}{P_{\mathrm{S}}\phi\left(a_1 - a_2\gamma_{\mathrm{th1}}\right)}, XZ > \frac{\gamma_{\mathrm{th1}}}{P_{\mathrm{S}}\phi\left(a_1 - a_2\gamma_{\mathrm{th1}}\right)} \right\}. \tag{12}$$

B. Probability that symbol x_2 cannot be decoded

In this NOMA system, the SIC technique is carried out at D_2 to remove the signal x_1 before detecting its own message.

We assume that the SIC is perfect at D_2 and denote $\mathrm{P}_{x_2}^{\mathrm{error}}$ as the event that the best relay or D_2 cannot decode the symbol x_2 correctly. Then, the expression of $\mathrm{P}_{x_2}^{\mathrm{error}}$ is given by

$$\begin{aligned} \mathrm{P}_{x_2}^{\mathrm{error}} &= \Pr\left(\min\left(\gamma_{1u2}, \gamma_{2u2}\right) \le \gamma_{\mathrm{th2}}\right) \\ &= 1 - \Pr\left(a_2 P_{\mathrm{S}} |h_{1,n}|^2 > \gamma_{\mathrm{th2}}, a_2 P_{\mathrm{R}} |g_2|^2 > \gamma_{\mathrm{th2}}\right). \end{aligned} \tag{18}$$

Substituting P_{R} from (3) into (18), we have

$$\mathrm{P}_{x_2}^{\mathrm{error}} = 1 - \Pr\left(X > \frac{\gamma_{\mathrm{th2}}}{a_2 P_{\mathrm{S}}}, Y > \frac{\gamma_{\mathrm{th2}}\left(1-\alpha\right)}{X 2 a_2 \alpha \eta P_{\mathrm{S}}}\right), \tag{19}$$

Based on the conditional probability [14], we can express (19) as

$$\mathrm{P}_{x_2}^{\mathrm{erro}} = 1 - \int_a^{\infty} \left[1 - F_Y\left(\frac{b}{x}\right)\right] f_X\left(x\right) dx, \tag{20}$$

where $a = \frac{\gamma_{\mathrm{th2}}}{a_2 P_{\mathrm{S}}}$ and $b = \frac{\gamma_{\mathrm{th2}}(1-\alpha)}{2 a_2 \alpha \eta P_{\mathrm{S}}}$.

By substituting the CDF and PDF of X and Y into (20) and then using expanded Taylor series, we obtain the expression of $\mathrm{P}_{x_2}^{\mathrm{error}}$ as in (21).

Similarly, when the transmitted power lies in a high region, it will lead to $a = \frac{\gamma_{\mathrm{th2}}}{a_2 P_{\mathrm{S}} \approx \infty} \to 0$. Hence, the approximation expression of $\mathrm{P}_{x_2}^{\mathrm{error}}$ is given by

$$\mathrm{P}_{x_2}^{\mathrm{erro}} \approx 1 - \sum_{n=1}^{N} \left(-1\right)^{n-1} \binom{N}{n} \sqrt{\frac{4bn}{\lambda_1 \lambda_3}} K_1\left(\sqrt{\frac{4bn}{\lambda_1 \lambda_3}}\right). \tag{22}$$

C. Imperfect SIC

We assume that both R and D_2 receive the imperfect SIC symbol x_1. Then, the SINRs at R and D_2 are respectively given as

$$\gamma_{1,u2} = \frac{a_2 P_{\mathrm{S}} |h_{1,n}|^2}{a_1 \rho_1 \mathrm{E}\{|x_1|^2\} P_{\mathrm{S}} |h_{1,n}|^2 + 1}, \tag{23}$$

$$\gamma_{2,u_2} = \frac{a_2 P_{\mathrm{R}} |g_2|^2}{a_1 \rho_2 \mathrm{E}\{|x_1|^2\} P_{\mathrm{R}} |g_2|^2 + 1}, \tag{24}$$

where $0 \le \rho_i \le 1$ with $i \in \{1, 2\}$ denotes the levels of residual interference due to the SIC imperfection at R and D_2. Especially, $\rho_i = 1$ and $\rho_i = 0$ refer to the cases of without SIC and perfect SIC, respectively.

In this case, it is considered that D_2 does not have the perfect knowledge of the signal information at D_1. Thus, the interference from D_1 cannot be perfectly removed at D_2. From (23) and (24), we have the outage probability expression shown in (25) on the top of the next page for the case of imperfect SIC x_1.

After solving (25), we get the result as

$$\mathrm{P}_{x_2}^{I-SIC\, x_1} = 1 - \int_c^{\infty} \left[1 - F_Y\left(\frac{d}{x}\right)\right] f_X\left(x\right) dx, \tag{26}$$

where $c = \frac{\gamma_{\mathrm{th2}}}{P_S(a_2 - a_1\rho_1\gamma_{\mathrm{th2}})}$ and $d = \frac{\gamma_{\mathrm{th2}}}{\phi P_S(a_2 - a_1\rho_2\gamma_{\mathrm{th2}})}$.

Then, with some further manipulations, we can rewrite (26) into (27).

In the high-power region, we have the approximation expression of $\mathrm{P}_{x_2}^{I-SIC\, x_1}$ as

$$\mathrm{P}_{x_2}^{I-SIC\, x_1} \approx 1 - \sum_{n=1}^{N} \left(-1\right)^{n-1} \binom{N}{n} \sqrt{\frac{4nd}{\lambda_1 \lambda_2}} K_1\left(\sqrt{\frac{4nd}{\lambda_1 \lambda_2}}\right). \tag{28}$$

IV. Simulation Results

In this section, several representative numerical results are provided to illustrate the impact of the number of relays, the channel gain (distance or path loss), and the imperfect SIC on the performance of NOMA systems with RF energy harvesting. The settings of system parameters are as follows. The distance from source S to D_1 is normalized to one unit. D_2 is closer to the relay node than D_1. The power allocation coefficient is $\frac{d_{D_1}^{-\mu}}{d_{R_n D_2}^{-\mu}} = \frac{a_2}{a_1}$ which is used to trade-off between the system throughput and the user fairness. $\mu \in \{2, ..., 6\}$ denotes the path loss coefficient of wireless environment [16]. The target rates $R_1 = 0.5$ $(bpcu)$ and $R_2 = 1$ $(bpcu)$, the energy harvesting fraction $\alpha = 0.3$. The channel gains $\lambda_{\mathrm{SR_n}} = \lambda_{\mathrm{R_n D_1}} = 1$ and $\lambda_{\mathrm{R_n D_2}} = 2$, and the efficiency coefficient of energy conversion $\eta = 1$.

Fig. 2 and Fig. 3 plot the outage performance of D_1 and D_2, respectively, versus the average SNR for the case of perfect SIC. In these scenarios, we consider the partial relay selection schemes in which the number of relays is varied. It is interesting to see from Fig. 2 and Fig. 3 that the performance gain is significant when increasing the number of relays from 1 to 3. It is because the selected best relay provides the best

$$\mathrm{P}_{x_2}^{\mathrm{error}} = 1 - \sum_{n=1}^{N} (-1)^{n-1} \binom{N}{n} \frac{n}{\lambda_1} \int_a^{\infty} \exp\left(-\frac{b}{\lambda_3 x}\right) \exp\left(-\frac{nx}{\lambda_1}\right) dx$$
$$= 1 - \sum_{n=1}^{N} (-1)^{n-1} \binom{N}{n} \frac{n}{\lambda_1} \sum_{k=0}^{N_t} \frac{(-1)^k}{k!} \left(\frac{b}{\lambda_3}\right)^k \left(\frac{1}{a}\right)^{k-1} E_k\left(\frac{na}{\lambda_1}\right). \quad (21)$$

$$\mathrm{P}_{x_2}^{I-SIC\,x_1} = \Pr\left[\min\left(\frac{a_2 P_{\mathrm{S}} |h_{1,n}|^2}{a_1 P_{\mathrm{S}} \rho_1 |h_{1,n}|^2 + 1}, \frac{a_2 P_{\mathrm{R}} |g_2|^2}{a_1 P_{\mathrm{R}} \rho_2 |g_2|^2 + 1}\right) \leq \gamma_{\mathrm{th2}}\right]. \quad (25)$$

$$\mathrm{P}_{x_2}^{I-SIC\,x_1} = 1 - \sum_{n=1}^{N} (-1)^{n-1} \binom{N}{n} \frac{n}{\lambda_x} \int_c^{\infty} \exp\left(-\frac{d}{\lambda_2 x}\right) \exp\left(-\frac{nx}{\lambda_1}\right) dx$$
$$= 1 - \sum_{n=1}^{N} (-1)^{n-1} \binom{N}{n} \frac{n}{\lambda_x} \sum_{k=0}^{N_t} \frac{(-1)^k}{k!} \left(\frac{d}{\lambda_2}\right)^k \left(\frac{1}{c}\right)^{k-1} E_k\left(\frac{nc}{\lambda_1}\right). \quad (27)$$

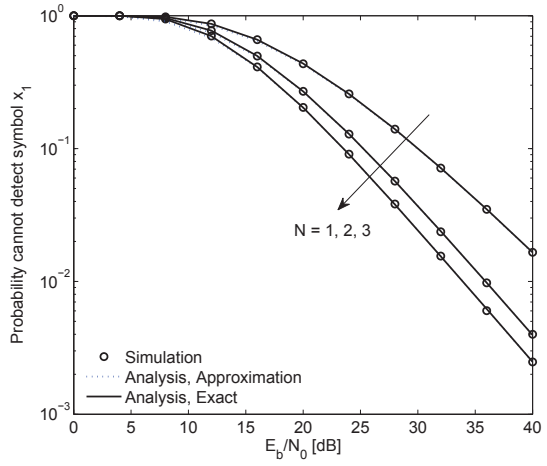

Fig. 2. Probability of decoding symbol x_1 unsuccessfully versus the average SNR with perfect SIC and different numbers of the relay nodes, N.

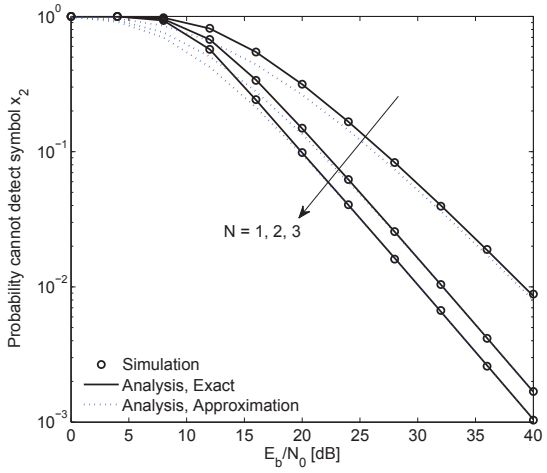

Fig. 3. Probability of decoding symbol x_2 unsuccessful versus the average SNR with perfect SIC and different numbers of the relay nodes, N.

channels from the source to relays so that better decoding performance as well as higher energy harvesting from the received RF signal from source S in the first phase can be achieved. We can see that the simulations results are in excellent agreement with the analytical results in all cases.

Fig. 4 shows the comparison of the outage performance of D_2 versus the average SNR for the cases of imperfect SIC and perfect SIC symbol x_1 with the levels of residual interference, ρ, at best relay and D_2 are $\rho_1 = 0.1$ and $\rho_2 = 0.4$, respectively. We should be reminded that D_1 only needs to decode symbol x_1 while D_2 has to correctly decode x_1 first, then uses SIC to obtain x_2. The probability of decoding the symbol x_2 unsuccessfully is plotted as a function of the average SNR in dB. The square markers and round markers indicate the simulation results of the perfect SIC and the imperfect SIC, respectively. From Fig. 4, we can see that the remaining coefficient SIC significantly impacts the performance of D_2. It is noticed that the simulation results are again in excellent agreement with the analytical results in all cases, which validates our mathematical models.

Next, we investigate the impact of energy harvesting coefficient on the probability of decoding symbol x_2 with different numbers of relay nodes, and present the results in Fig. 5. In this scenario, we assume that SIC symbol x_1 is perfect and the transmitted power from the source is $P_{\mathrm{S}} = 20$ dB. As shown in Fig. 5, the minimum value of the unsuccessful

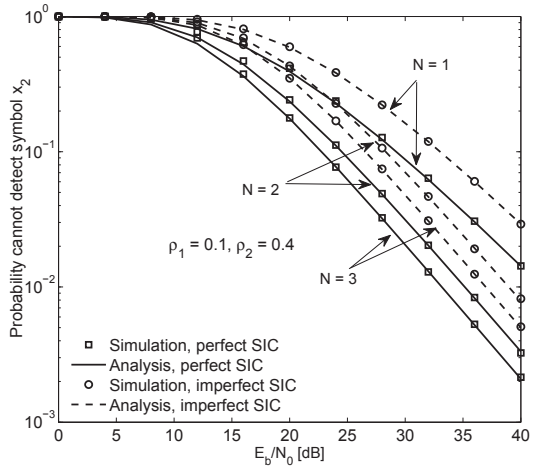

Fig. 4. Comparison of the outage performance of D_2 versus the average SNR for the cases of imperfect SIC and perfect SIC x_1 with $\rho_1 = 0.1$ at the best relay and $\rho_2 = 0.4$ at D_2.

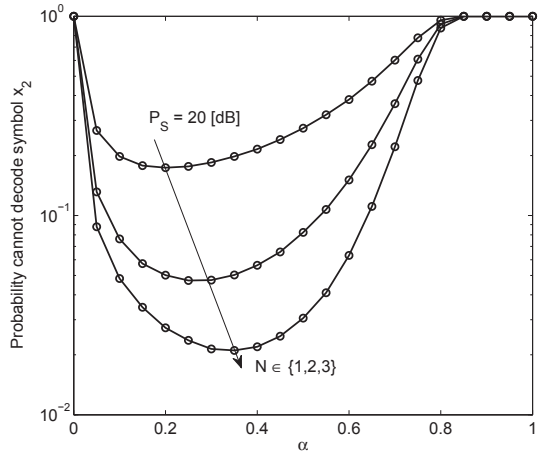

Fig. 5. Impact of the number relay nodes on the time frame energy harvesting and information processing.

symbol x_2 is different and depends on the number of relay nodes, N. When N increases, the time frame for information processing decreases, leading to an improvement in the amount of harvested energy (refer to (2)).

V. Conclusions

In this paper, we analyze the influence of energy harvesting technique in NOMA relaying networks. Partial relay selection scheme is applied to improve the system performance. The closed-form expressions of the probabilities of unsuccessful decoding symbol x_1 and x_2 are derived. We also compare the outage performance in both cases of perfect SIC and imperfect SIC. These analysis expressions are verified by the Monte Carlo simulation method. From the theoretical and simulation results, some important conclusions can be summarized as follows. 1) The system performance and the amount of harvested energy are improved with the increase in the number of relay nodes, N. 2) Unlike previous works in the literature, we investigate the adaptation of power allocation coefficient versus the channel gain. 3) The presented simulation results verify the correctness of our mathematical analysis. As future works, we will apply NOMA into the multiple-relay multiple-antenna EH relaying networks and analyze the network performance over Nakagami-m fading channel or double Rayleigh fading channel. In addition, we will investigate the impact of the imperfect CSI on the performance of relay selection method.

Acknowledgment

This work was supported by the National Research Foundation of Korea (NRF) grant funded by the Korea government (MSIP) (No. NRF-2015R1A2A2A03004152).

References

[1] Y. Wang, B. Ren, S. Sun, S. Kang, and X. Yue, "Analysis of Non-Orthogonal Multiple Access for 5G," *China Commun.*, vol. 13, no. Supplement No. 2, pp. 52–66, 2016.

[2] L. Dai, B. Wang, Y. Yuan, S. Han, I. Chih-Lin, and Z. Wang, "Non-Orthogonal Multiple Access for 5G: Solutions, Challenges, Opportunities, and Future Research Trends," *IEEE Commun. Mag.*, vol. 53, no. 9, pp. 74–81, Sep. 2015.

[3] S. Luo and K. C. Teh, "Adaptive Transmission for Cooperative NOMA System with Buffer-Aided Relaying," *IEEE Commun. Lett.*, vol. 21, no. 4, pp. 937–940, Jan. 2017.

[4] M. F. Kader, M. B. Shahab, and S.-Y. Shin, "Exploiting Non-orthogonal Multiple Access in Cooperative Relay Sharing," *IEEE Commun. Lett.*, vol. 21, no. 5, pp. 1159–1162, Jan. 2017.

[5] C. Du, X. Chen, and L. Lei, "Energy-Efficient Optimisation for Secrecy Wireless Information and Power Transfer in Massive MIMO Relaying Systems," *IET Commun.*, vol. 11, no. 1, pp. 10–16, Dec. 2017.

[6] R. Sun, Y. Wang, X. Wang, and Y. Zhang, "Transceiver Design for Cooperative Non-Orthogonal Multiple Access Systems with Wireless Energy Transfer," *IET Commun.*, vol. 10, no. 15, pp. 1947–1955, Oct. 2016.

[7] W. Han, J. Ge, and J. Men, "Performance Analysis for NOMA Energy Harvesting Relaying Networks with Transmit Antenna Selection and Maximal-ratio Combining over Nakagami-*m* Fading," *IET Commun.*, vol. 10, no. 18, pp. 2687–2693, Dec. 2016.

[8] Y. Liu, Z. Ding, M. Elkashlan, and H. V. Poor, "Cooperative non-orthogonal multiple access with simultaneous wireless information and power transfer," *IEEE J. Sel. Areas Commun.*, vol. 34, no. 4, pp. 938–953, Mar. 2016.

[9] K. I. Pedersen, T. E. Kolding, I. Seskar, and J. M. Holtzman, "Practical Implementation of Successive Interference Cancellation in DS/CDMA Systems," in *Proc. of 1996 5th IEEE International Conference on Universal Personal Communications*. IEEE, Aug. 1996, pp. 321–325.

[10] Y. Gu and S. Aïssa, "RF-based Energy Harvesting in Decode-and-Forward Relaying Systems: Ergodic and Outage Capacities," *IEEE Trans. Commun.*, vol. 14, no. 11, pp. 6425–6434, Jul. 2015.

[11] D. S. Michalopoulos, H. A. Suraweera, and R. Schober, "Relay Selection for Simultaneous Information Transmission and Wireless Energy Transfer: A Tradeoff Perspective," *IEEE J. Sel. Areas Commun.*, vol. 33, no. 8, pp. 1578–1594, Jan. 2015.

[12] A. Benjebbour, K. Saito, A. Li, Y. Kishiyama, and T. Nakamura, "Non-Orthogonal Multiple Access (NOMA): Concept and Design," *Signal Proces. for 5G: Algorithms and Implementations*, pp. 143–168, Aug. 2016.

[13] Z. Yang, Z. Ding, P. Fan, and N. Al-Dhahir, "The Impact of Power Allocation on Cooperative Non-Orthogonal Multiple Access Networks with SWIPT," *IEEE Trans. Commun.*, vol. 16, no. 7, pp. 4332–4343, May 2017.

[14] A. Papoulis and S. U. Pillai, *Probability, Random Variables, and Stochastic Processes*. Tata McGraw-Hill Education, 2002.

[15] D. Zwillinger, *Table of Integrals, Series, and Products*. Elsevier, 2014.

[16] A. Goldsmith, *Wireless Communications*. Cambridge university press, 2005.